



## RESEARCH ARTICLE

# Directional beaming of surface plasmon polaritons from a metallic nanochannels with defected surface cavity

A. Mudhafer<sup>1</sup> | Raed M. Shaaban<sup>2</sup> | Diyah K. Shary<sup>3</sup>

<sup>1</sup>Chemical and Petrochemical Technical Engineering Department, Southern Technical University, Basrah, Iraq

<sup>2</sup>Physics Department, Faculty of Science, University of Basrah, Basrah, Iraq

<sup>3</sup>Electrical Power Technical Engineering Department, Southern Technical University, Basrah, Iraq

## Correspondence

A. Mudhafer, Chemical and Petrochemical Technical Engineering Department, Southern Technical University, Iraq.  
Email: a.mudhafer@stu.edu.iq

## Abstract

In this paper, the directional excitation of surface plasmon polarities (SPPs) was investigated with numerical simulations in two plasmonic structures based on the metallic nanochannels with bumps. The simulation of SPPs and directional propagating fields on the output interface was carried out by employing a finite element method implemented by COMSOL Multiphysics. By analyzing behavior of the instantaneous electric field and power flow, the introduction of dielectric-metal (DM) bumps produced an enhancement of the directionality and confinement of the output field in comparison with the case of metallic bumps. Since the DM bumps can form the vertical MDM Fabry-Pérot (FP) cavity modes which are coupling with FP surface cavity modes between two bumps. The simulation results show that the optimized FP cavity length, dielectric thickness of layer in DM bumps and dielectric thickness of the layer between two bumps is crucial for the enhancement of the directional beaming effects. It is hoped that these outcomes can be used in several potential applications such as directional coupler (generator), plasmonic circuits, and nano-resolution optical beaming.

## KEYWORDS

beaming effects, instantaneous field, nanochannels, power flow, SPPs

## 1 | INTRODUCTION

Striving for the progress in nanofabrication technology has become the standard impulse and the conventional topic for the introductory paragraphs for most researches are dealing with nanophotonic devices, that are of fundamental or engineering character, experimental<sup>1-3</sup> or theoretical.<sup>4-6</sup> The optical diffraction limit acts as an obstacle to the downscaling of photonic devices. One approach to conquer this case is the utilization of the properties of surface plasmon polaritons (SPPs).<sup>7</sup> SPPs are electromagnetic waves coupled to the free electron oscillation on the metal surface and strongly confined to the near vicinity of the dielectric-metal interface with amplitudes evanescently decaying perpendicular to the interface of metal and a dielectric, leading to an enhancement of the electromagnetic field at the interface or resulting in extraordinary sensitivities to surface conditions.<sup>8-11</sup> Owing to the above points, SPPs are suitable for various applications. For example, optical beaming,<sup>12,13</sup> filters,<sup>14,15</sup> optical logic gates,<sup>16,17</sup> sensors,<sup>18-24</sup> and waveguides<sup>25,26</sup> and that is just to name a few. In the visible spectrum region, the SPPs wavelength  $\lambda_{\text{SPP}}$  is slightly less than the free space wavelength  $\lambda_0$ . This light-SPPs decoupling means that light cannot convert directly to SPPs on a planar surface.<sup>27</sup> In the plasmonic nanoscale structures and devices, the nanoslit is generally utilized to excite SPPs because it is a small dimension and efficient light-SPPs coupling.<sup>28-31</sup> The light diffracts uniformly into all directions when it propagates through a nanoslit. Thus, this phenomenon lays a lower restriction on the dimension of photonic devices in applications. To collect electromagnetic energy efficiently, an ultra-compact highly directional beaming device is required. In fact, in many applications, it is desired to convert SPPs into a freely directional propagating field. Many studies have mainly focused on investigating the phenomenon of beaming or directionality of light. A simplified model of slit-bump<sup>32</sup> and subwavelength aperture,<sup>33</sup> are applied to understand the physical mechanism behind this phenomenon. Meanwhile, periodic surface corrugation at the output interface of metallic slit has also been widely studied.<sup>34,35</sup> Most recently, the proposed configurations such as implanted nanogrooves,<sup>36</sup> metasurfaces,<sup>37</sup> array of nanoslits,<sup>38</sup> and metalens<sup>39</sup> are aiming to enhance the directional beaming effects, which are particularly focused on the study of shape, size and periodicity of a metallic slit and array of nanoslits with straight channel. Despite the fact that SPPs have an essential role in beaming light, there is still a necessity for inclusive investigations into this phenomenon, especially the

introduction of nanoslits with shaped channels and various configurations of bumps at the output interface, which represented surface defects that altered surface morphology. Herein, the present study employs numerical simulations dependent on finite element method (FEM) to further investigate the phenomenon of directional beaming in the plasmonic nanostructures consisting of the metallic nanochannels with two pumps. To observe this phenomenon of the proposed structures, the distributions of an instantaneous electric field and power flows are analyzed in detail. The present study highlights a considerable contribution of the bumps configurations at output of metal surface, in the enhancement of beam directionality which provide effective way of light-SPPs coupling and then constituting different kinds of Fabry-Pérot (FP) cavities. Furthermore, this investigation contributes to the increasing knowledge on the SPPs signal features such as distribution of instantaneous electric field, field confinement, and power flow carried by SPPs, which are significant in real applications of SPPs. The remainder of this paper is organized as follows: the simulation structures and physical mechanisms for directional excitation of SPPs are outlined in Section 2. The obtained results are presented and discussed in Section 3. The paper is concluded in Section 4.

## 2 | SIMULATION STRUCTURES AND METHODS

Diagrammatic sketch of the proposed structures is shown in Figure 1. The structural geometries are divided into the following: first is a metallic nanostructure composed of two symmetric U-shaped metallic nanochannels (U-shaped and upside down U-shaped) which are connected by a central connecting channel, where the two bumps stand at the output interface. The dielectric layer covers the top of the metal surface in the region between the two bumps. Based on the first structure (Figure 1A), the second structure in Figure 1B is designed, where dielectric-metal DM bumps are introduced instead of metallic bumps. For simplicity, the above two structures are pointed “structure 1” and “structure 2”, respectively. The structures are illuminated normally by a plane wave of TM polarization (the magnetic field perpendicular to the  $x$ - $z$  plane) with wavelength  $\lambda_0 = 500$  nm.

The coordinate origin is set at the center of distance between the nanochannels at output side. The geometries are defined by the following parameters: the height and width of side channels (central connecting channel) are  $H_1$  ( $H_2$ ) and  $W_1$  ( $W_2$ ), respectively. The width of the nanochannels is less than half of the incidence light wavelength ( $\lambda_0/2$ ), which controls the near field effects at the nanochannels. The distance between the two bumps is defined as  $d$ . The height and width of bumps are  $H_3$  and  $W_3$ , respectively. The dielectric layer on the top of metal surface with a thickness of  $H_{d1}$  and the dielectric layer of DM bumps with a thickness of  $H_{d2}$

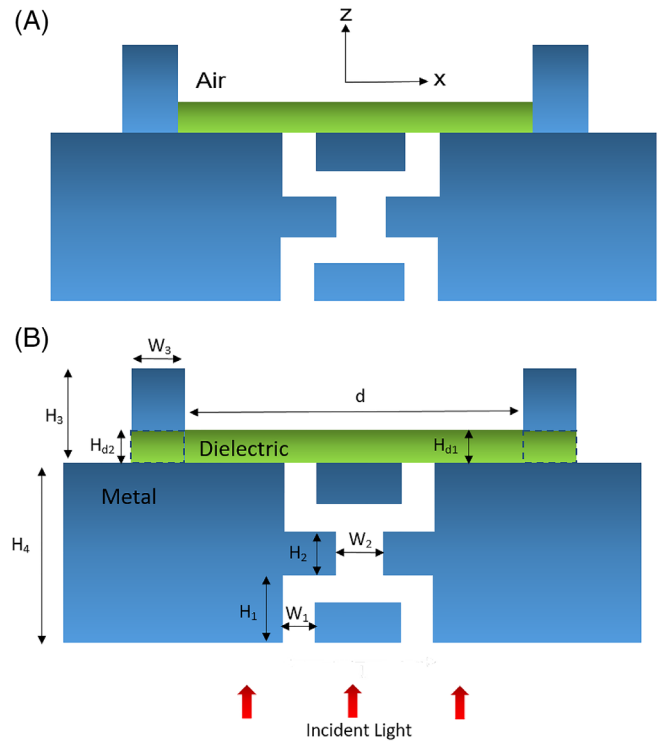


**FIGURE 1** Schematic configuration of proposed nanostructures (A) metallic nanochannels with bumps (structure 1) (B) metallic nanochannels with DM bumps (structure 2). The plane wave of TM polarization is normally an incident from the bottom [Color figure can be viewed at [wileyonlinelibrary.com](http://wileyonlinelibrary.com)]

consist of  $\text{SiO}_2$  with refractive index of  $n = 1.46$ .<sup>40</sup> The proposed structures are constructed of a silver (Ag) film which is a dependable plasmonic material in the visible spectrum and usually utilized for fabrication of optical nanostructures.<sup>41</sup> The thickness of the Ag film  $H_4$  which contains nanochannels is more than the skin depth ( $\sim 26.85$  nm) of the Ag film. The optical material properties of Ag are described by<sup>40</sup> where the wavelength dependent permittivity value of  $-7.632 + 0.730i$  at  $\lambda_0 = 500$  nm is used. Most of Ag and  $\text{SiO}_2$  properties are available in COMSOL Multiphysics material library. In this FEM simulation model, the scattering boundary conditions are applied at the outsider boundaries. Notably, the physical mechanism of the directional excitation of SPPs in the proposed structures is described as follows: under the normal incident of electromagnetic plane wave, the SPPs can be excited at the input and output sides of the nanochannels. A portion of electromagnetic mode couples into propagating mode in the nanochannels. The light emerging from the nanochannels on the output side includes radiating and evanescent modes (ie, SPPs mode). The SPPs exiting the nanochannels propagate towards the two bumps will be backscattered due to the bumps reflection. The reflected SPPs will interfere with directly emanating from the nanochannels. Thus, there are two kinds of FP cavities for SPPs modes based on MDM structure. One is a surface cavity which is formed between

two bumps in the lateral dimension of both structures, and other is a vertical MDM cavity which is formed by DM bumps in structure 2. Accordingly, the proposed structures would act as an efficient source of directional SPPs coupler.

### 3 | SIMULATION RESULTS AND ANALYSIS

The simulation results of the finite elements method FEM present an intriguing phenomenon taking place instantaneously for the appropriate surface FP cavity length  $d$ . The SPPs are converted into a directional collimated beams and their directions are determined by the geometry parameters of the structures. To observe this phenomenon of structure 1 and structure 2, the behavior of normalized instantaneous electric field is shown in Figure 2 with different surface FP cavity lengths  $d$  where  $d = 470, 940, 1410,$  and  $1880$  nm depicted in Figure 2A-D, E-H, respectively. Figure 2A-D, E-H corresponds to the structure 1 and 2, respectively.

In Figure 2, extra symmetric beams are emerging at the output interface with both directions of propagation for SPPs when the increment of the cavity length  $d$  is about  $\lambda_{\text{SPP}} = 470$  nm. However, comparing the results in Figure 2, it is clear that the directional beaming effects in structure 2 corresponding to Figure 2E-H are much stronger than in structure 1 corresponding to Figure 2A-D. Intriguingly, in Figure 2E-H, the number of extra symmetric beams, which emerged at the output interface, increased significantly by increasing  $d$  by  $\lambda_{\text{SPP}}$ . The enhancement of the directional beaming effects in structure 2 is mainly due to the introduction of the DM bumps which form two vertical MDM cavities over the metal surface. Thus, their modes are coupling with surface FP cavity modes. To further buttress the above

observation, normalized instantaneous electric field intensity at distance of 400 nm above the metal surface along the  $x$ -axis was calculated with different values of cavity lengths  $d$ . Figure 3A,B shows the results corresponds to the structure 1 and 2, respectively.

In Figure 3B, the output field gains directionality with confinement along the surface stronger than in Figure 3A. Also in Figure 3B, the intensity at optimized value  $d = 470$  nm is around 1.08-times higher than Figure 3A at optimized value  $d = 1410$  nm. Obviously, this enhancement in structure 2 clarifies that a vertical MDM cavity presence efficiently increases the intensity which was discussed previously. However, for all cavity lengths  $d$  as shown in Figure 3A,B the greatest portion of the field is diffracted rather than confined in the propagating direction. The simulation results show that the instantaneous electric field intensity in structure 2 depends on the bumps configurations and thickness of  $\text{SiO}_2$  layer  $H_{d2}$  in bumps. Figure 4A,B displays the dependence of normalized instantaneous electric field intensity on the bumps configurations and thickness  $H_{d2}$ , at distance of 400 nm above the metal surface, respectively.

In Figure 4A, there are two cases of the bumps configurations in structure 2: DM bumps and MD bumps. The employment of DM bumps provides the most directional, confined, and high intensity beam than MD bumps. The output electric field intensity due to DM bumps (in blue color) is 1.15-times higher than due to the MD bumps (in red color), respectively. This is due to the presence of a vertical MDM cavity, while there is only one surface cavity (between two bumps) in presence of MD bumps without a vertical MDM cavity. In Figure 4B, the directionality of the output electric field is decreased when  $H_{d2}$  is increased and vice versa for the confinement field. At  $H_{d2} = 50$  nm the

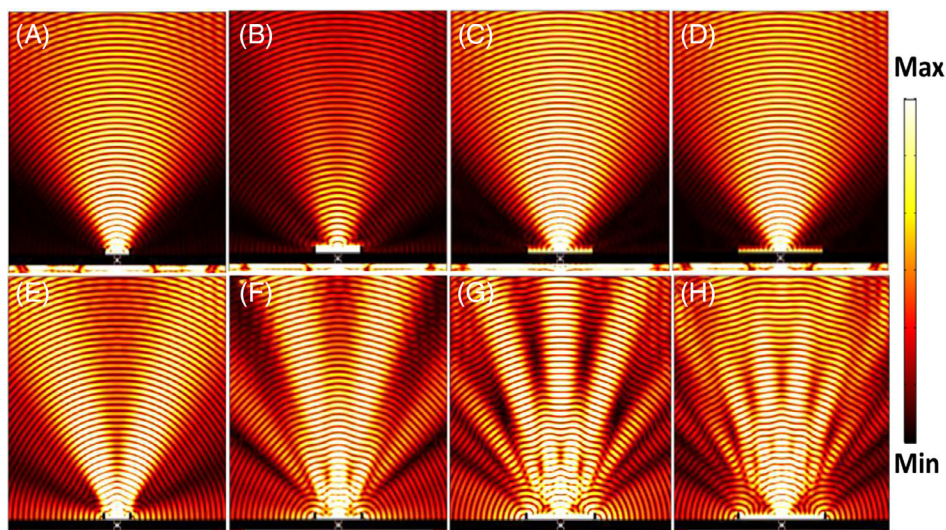


**FIGURE 2** Distribution of normalized instantaneous electric field at different values of  $d$ . In both structures  $L, W_1, W_3, H_1, H_2, H_3,$  and  $H_{d1}$  are taken as 200, 50, 100, 150, 100, 300, and 50 nm, respectively. The value of  $W_2$  in structures 1 and 2 are taken as 150 and 200 nm, respectively. In structure 2,  $H_{d2}$  is taken as 50 nm [Color figure can be viewed at [wileyonlinelibrary.com](http://wileyonlinelibrary.com)]

directionality (confinement) approaches to its maximum (minimum), respectively. When  $H_{d2} = H_3 = 300$  nm the bumps will be completely filled with a  $\text{SiO}_2$  thus, the

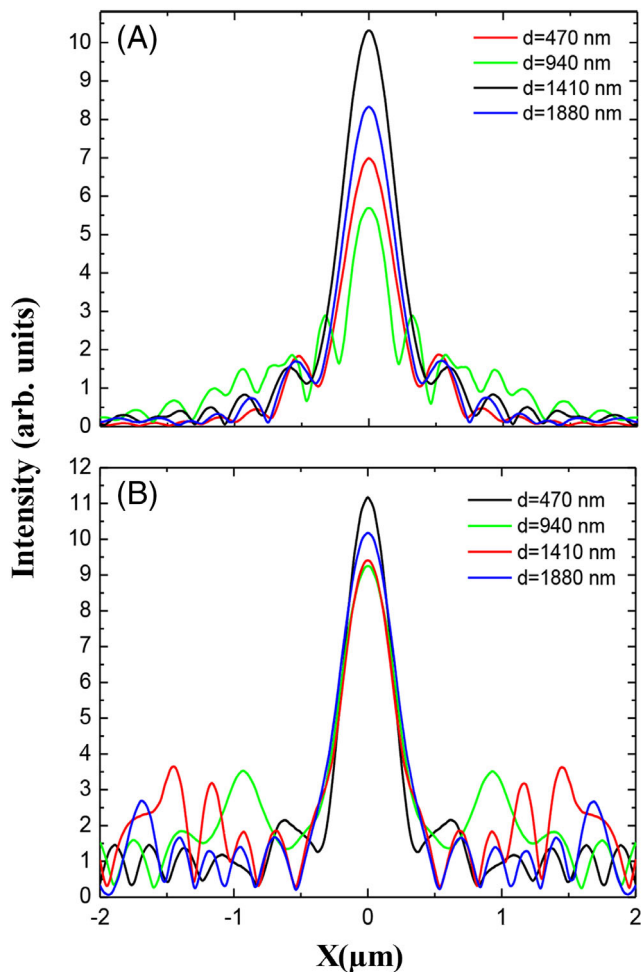


**FIGURE 3** The output electric field intensity at distance of 400 nm above the metal surface with different values of  $d$  for structures 1 (A) and 2 (B). All geometrical parameters are the same as those in Figure 2 [Color figure can be viewed at [wileyonlinelibrary.com](http://wileyonlinelibrary.com)]

directionality (confinement) it has minimum (maximum) value. In other words, the DM bumps will become completely dielectric bumps without surface defect cavities. Its well-known that the variation in the thicknesses of the dielectric layer  $H_{d1}$  on the metal surface enables tuning of the efficiency of the nanochannels coupling to SPPs, so the distribution of the power flows on the output side of nanochannels is sensitive to  $H_{d1}$ . To explore the influence of  $H_{d1}$  on the distribution of normalized time-averaged power flows at different  $H_{d1}$  where  $H_{d1} = 50, 150, 200$  and  $300$  nm depicted in Figure 5A-D, E-H, respectively. Figure 5A-D, E-H corresponds to the structure 1 and 2, respectively.

With respect to structure 1, at  $H_{d1} = 50$  nm (Figure 5A) the power flow reaches its maximum and the behavior of it is approximately same behavior at  $H_{d1} = 200$  nm (Figure 5C). At  $H_{d1} = 150$  nm and  $H_{d1} = 300$  nm (Figure 5B,D) most of the power flow is confined to the near vicinity of the nanochannels between two bumps. To some extent, the power flow reaches directionality and nevertheless it stills rather weak and the beam is split into fragments. This behavior is clearer at  $H_{d1} = H_3 = 300$  nm (Figure 5D), where the region between bumps is completely covered by  $\text{SiO}_2$ . Introduced DM bumps in structure 2 (Figure 5E-H) produce relatively higher directionality of the power flow compared with structure 1. It is noticeable that  $H_{d1} = 50$  and  $H_{d1} = 300$  nm (Figure 5E,H) give the strongest power flow in the propagating direction with higher light confining effect in case of  $H_{d1} = 50$  nm than  $H_{d1} = 300$  nm. At  $H_{d1} = 150$  nm (Figure 5F) the power flow is not behaving like a beam but rather it is diffracted on the output side of the nanochannels and most of the power flow is confined along the surface, while in the case of  $H_{d1} = 200$  nm (Figure 5G) the power flow is akin to Figure 5E but it has a slight directionality and the large portion of it is confined along the surface. Motivated by the results in Figure 5, Figure 6 shows the distribution of normalized power flows at 400 nm above the metal surface with different values of

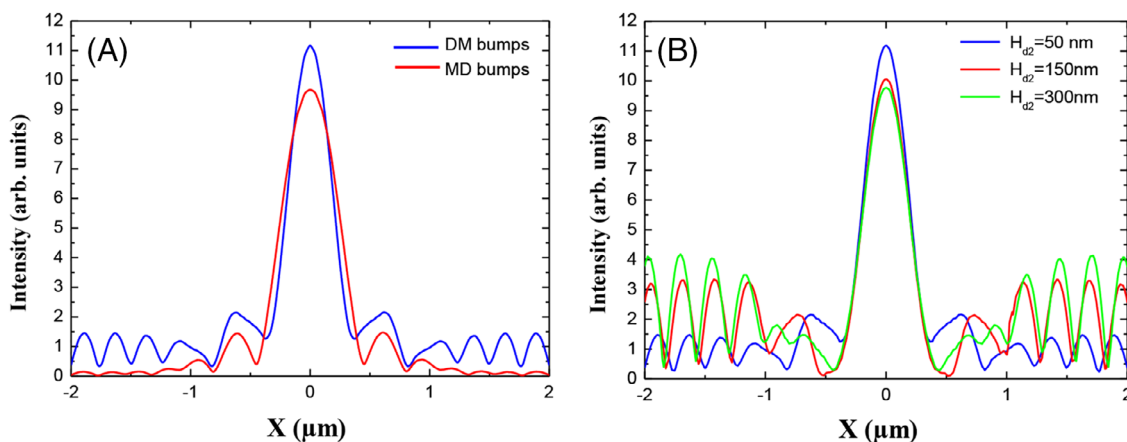


**FIGURE 4** Dependence of the output electric field intensity on the bumps configuration (A) and thickness  $H_{d2}$  (B).  $d$  and  $W_2$  are taken as 470 and 150 nm, respectively, and the other geometrical parameters are the same as those in Figure 2 [Color figure can be viewed at [wileyonlinelibrary.com](http://wileyonlinelibrary.com)]

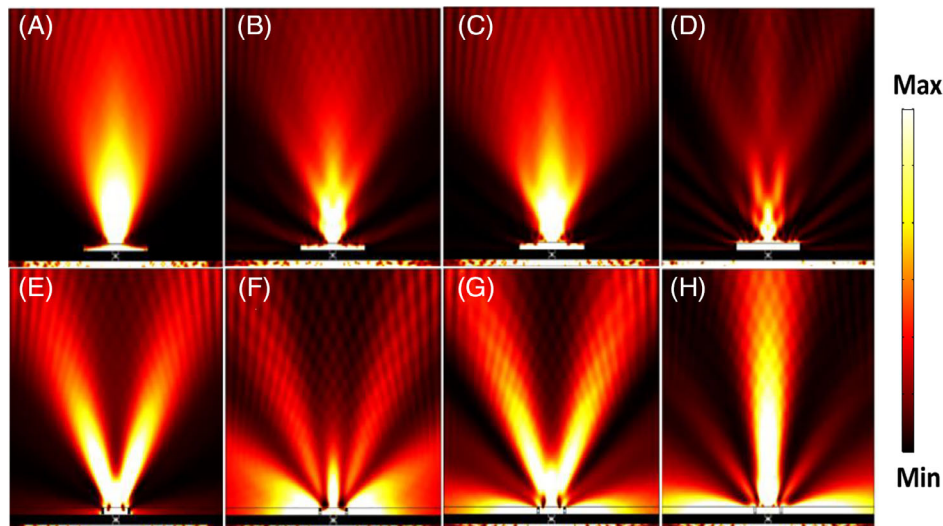


**FIGURE 5** Distribution of normalized time-averaged power flow at different values of  $H_{d1}$  for structures 1 (A–D) and 2 (E–H). For structure 1 (structure 2) the values of  $d$  and  $W_2$  are taken as 1410 nm (470 nm) and 200 nm (150 nm), respectively, and the other geometrical parameters are the same as those in Figure 2 [Color figure can be viewed at [wileyonlinelibrary.com](http://wileyonlinelibrary.com)]

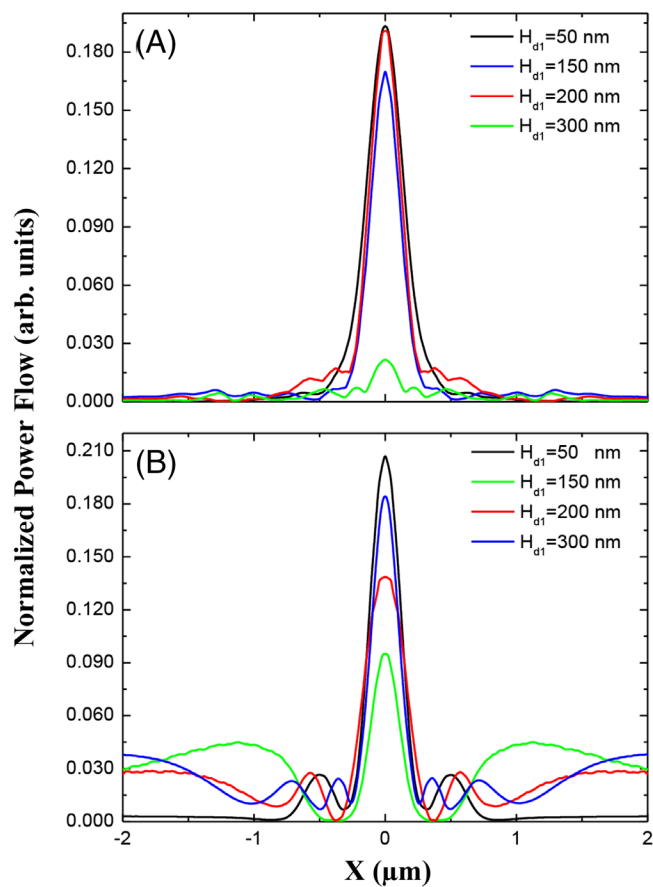


**FIGURE 6** Distribution of normalized power flows at 400 nm above surface at different values of  $H_{d1}$  for structures 1 (A) and 2 (B).  $d$  and  $W_2$  are taken as 1410 nm (470 nm) and 200 nm (150 nm) for structure 1 (structure 2), respectively and the other geometrical parameters are the same as those in Figure 2 [Color figure can be viewed at [wileyonlinelibrary.com](http://wileyonlinelibrary.com)]

$H_{d1}$ . Figure 6A,B corresponds to the structure 1 and 2, respectively. In Figure 6A,B, at the optimized value of  $H_{d1} = 50$  nm, the power flow in structure 2 is around 1.07-times higher than in structure 1. The previous reasons are sufficient to interpret the results in Figure 6.

## 4 | CONCLUSIONS

The directional excitation of SPPs is numerically investigated in two plasmonic structures. The two structures that are proposed and simulated consist of a metallic nanochannels with two bumps, where the dielectric layer which covers the region between two bumps (structure 1). Depending on the structure 1, the structure 2 is designed by replacing the two bumps with DM bumps. There are two kinds of FP surface cavities formed, one is the surface cavity in lateral dimension (structure 1) and the other is lateral surface cavity with a vertical MDM cavity (structure 2). The simulation results show that the directional beaming effects in structure 2 with DM bumps are enhanced in comparison with those in structure 1. DM bumps could further improve directionality and the confined field, owing the coupling between lateral and vertical MDM cavities modes. By optimizing the surface cavity length, thickness of dielectric layer for DM bumps and thickness of dielectric layer between two bumps, the directional beaming effects can achieve enhancement. It is expected that the recent results may be utilized in several applications such as directional coupler (generator), plasmonic circuits, and nanoresolution optical beaming.

## ACKNOWLEDGMENTS

We acknowledge Ra'ed Malallah and Zahraa S. Khaleel for their helpful discussions.

## ORCID

A. Mudhafer  <https://orcid.org/0000-0002-6966-4329>

## REFERENCES

- [1] Maier S. Plasmonics: clear for launch. *Nat Phys.* 2007;3(5):301-302.
- [2] Yao K, Unni R, Zheng Y. Intelligent nanophotonics: merging photonics and artificial intelligence at the nanoscale. *Nano.* 2019;8(3):339-366.
- [3] Tischler N, Fernandez-Corbaton I, Zambrana-Puyalto X, et al. Experimental control of optical helicity in nanophotonics. *Light Sci Appl.* 2014;3(6):e183.
- [4] Zhou Z, Wu H, Feng J, Hou J, Yi H, Wang X. Silicon nanophotonic devices based on resonance enhancement. *J Nanophoton.* 2010;4(1):041001.
- [5] Jia L, Thomas EL. Theoretical study on photonic devices based on a commensurate two-pattern photonic crystal. *Opt Lett.* 2011;36(17):3416-3418.
- [6] Holmström P, Yuan J, Qiu M, Thylén L, Bratkovsky AM. Theoretical study of nanophotonic directional couplers comprising near-field-coupled metal nanoparticles. *Opt Express.* 2011;19(8):7885-7893.
- [7] Ebbesen TW, Lezec HJ, Ghaemi HF, Thio T, Wolff PA. Extraordinary optical transmission through sub-wavelength hole arrays. *Nature.* 1998;391(6668):667-669.
- [8] Raether H. *Surface Plasmons on Smooth Surfaces.* In surface plasmons on smooth and rough surfaces and on gratings (pp. 4-39). Berlin, Heidelberg: Springer; 1988.
- [9] Kirchain R, Kimerling L. A roadmap for nanophotonics. *Nat Photon.* 2007;1(6):303-305.
- [10] Maier SA, Brongersma ML, Kik PG, Meltzer S, Requicha AA, Atwater HA. Plasmonics—a route to nanoscale optical devices. *Adv Mater.* 2001;13(19):1501-1505.
- [11] Tuchscherer P, Rewitz C, Voronine DV, de Abajo FJG, Pfeiffer W, Brixner T. Analytic coherent control of plasmon propagation in nanostructures. *Opt Express.* 2009;17(16):14235-14259.
- [12] Hwang Y, Yang JK. Directional coupling of surface plasmon polaritons at complementary split-ring resonators. *Sci Rep.* 2019;9(1):7348.
- [13] Li H, Xu Y, Wang G, Fu T, Wang L, Zhang Z. Converting surface plasmon polaritons into spatial bending beams through graded dielectric rectangles over metal film. *Opt Commun.* 2017;383:423-429.
- [14] Mirmaziry SR, Setayesh A, Abrishamian MS. Design and analysis of plasmonic filters based on stubs. *JOSA B.* 2011;28(5):1300-1307.
- [15] Wang A, Dan Y. Mid-infrared plasmonic multispectral filters. *Sci Rep.* 2018;8(1):11257.
- [16] Abdulnabi SH, Abbas MN. Design an all-optical combinational logic circuits based on nano-ring insulator-metal-insulator plasmonic waveguides. *Photonics.* 2019;6(1):30.
- [17] Dolatabady A, Granpayeh N. All optical logic gates based on two dimensional plasmonic waveguides with nanodisk resonators. *J Opt Soc Korea.* 2012;16(4):432-442.
- [18] López-Muñoz GA, Estevez MC, Peláez-Gutiérrez EC, et al. A label-free nanostructured plasmonic biosensor based on Blu-ray discs with integrated microfluidics for sensitive biodetection. *Bio-sens Bioelectron.* 2017;96:260-267.
- [19] Jin XP, Huang XG, Tao J, Lin XS, Zhang Q. A novel nanometric plasmonic refractive index sensor. *IEEE Trans Nanotechnol.* 2010;9(2):134-137.
- [20] Chen J, Fan W, Mao P, et al. Tailoring plasmon lifetime in suspended nanoantenna arrays for high-performance plasmon sensing. *Plasmonics.* 2017;12:529-534.
- [21] Chen J, Fan W, Zhang T, et al. Engineering the magnetic plasmon resonances of metamaterials for high-quality sensing. *Opt Exp Dermatol.* 2017;25:3675-3681.
- [22] Chen J, Nie H, Cheng P, et al. Enhancing the magnetic Plasmon resonance of three-dimensional optical metamaterials via strong coupling for high-sensitivity sensing. *J Lightwave Technol.* 2018;36(3481-3485):3481-3485.
- [23] Chen J, Nie H, Zha T, et al. Optical magnetic field enhancement by strong coupling in metamaterials. *J Lightwave Technol.* 2018;36(2791-2795):2791-2795.
- [24] Chen J, Yuan J, Zhang Q, et al. Dielectric waveguide-enhanced localized surface plasmon resonance refractive index sensing. *Opt Mater Express.* 2018;8:342-347.
- [25] Fang Y, Sun M. Nanoplasmonic waveguides: towards applications in integrated nanophotonic circuits. *Light Sci Appl.* 2015;4(6):e294.
- [26] Gramotnev DK, Vernon KC, Pile DFP. Directional coupler using gap plasmon waveguides. *Appl Phys B Lasers Opt.* 2008;93(1):99-106.
- [27] Barnes WL. Surface plasmon-polariton length scales: a route to sub-wavelength optics. *J Opt A Pure Appl Opt.* 2006;8(4):S87-S93.
- [28] Gan Q, Guo B, Song G, et al. Plasmonic surface-wave splitter. *Appl Phys Lett.* 2007;90(16):161130.
- [29] Gan Q, Fu Z, Ding YJ, Bartoli FJ. Bidirectional subwavelength slit splitter for THz surface plasmons. *Opt Express.* 2007;15(26):18050-18055.
- [30] López-Tejiera F, Rodrigo SG, Martín-Moreno L, et al. Efficient unidirectional nanoslit couplers for surface plasmons. *Nat Phys.* 2007;3(5):324-328.
- [31] López-Tejiera F, Rodrigo SG, Martín-Moreno L, et al. Modulation of surface plasmon coupling-in by one-dimensional surface corrugation. *New J Phys.* 2008;10(3):033035.
- [32] Yong-Liang Z, De-Yin Z, Chuan-Hong Z, Xun-Ya J. Directional nanoslit-bump coupler for surface plasmon polaritons. *Chin Phys Lett.* 2008;25(1):168-171.
- [33] Lezec HJ, Degiron A, Devaux E, et al. Beaming light from a sub-wavelength aperture. *Science.* 2002;297(5582):820-822.
- [34] Zhang Y, Zhao D, Zhou C, Jiang X. Directional light emission through a metallic nanostructure. *J Appl Phys.* 2009;105(11):113124.
- [35] Liu Y, Shi H, Wang C, Du C, Luo X. Multiple directional beaming effect of metallic subwavelength slit surrounded by periodically corrugated grooves. *Opt Express.* 2008;16(7):4487-4493.

- [36] Daniel S, Bawuah P. Plasmonic implanted Nanogrooves for optical beaming. *Sci Rep.* 2019;9(1):391.
- [37] Zhu H, Yin X, Chen L, Li X. Directional beaming of light from a subwavelength metal slit with phase-gradient metasurfaces. *Sci Rep.* 2017;7(1):12098.
- [38] Nasari H, Abrishamian MS. Beam manipulating via an array of nanoslits modified by perpendicular cuts and bumps. *Plasmonics.* 2013;8(4):1675-1682.
- [39] Zhao K, Zhang H, Fu Y, Zhu S. Specialized directional beaming through a metalens and a typical application. *Nano.* 2018;7(1):339-345.
- [40] Edward, D. P., & Palik, I. (1985). *Handbook of Optical Constants of Solids.* Orlando, Florida: Academic Press.
- [41] Wiley, B. J., Im, S. H., Li, Z. Y., McLellan, J., Siekkinen, A., & Xia, Y. (2006). Maneuvering the Surface Plasmon Resonance of Silver Nanostructures through Shape-Controlled Synthesis. *J Phys Chem B.* 2006;110(32):15666–15675.

**How to cite this article:** Mudhafer A, Shaaban RM, Shary DK. Directional beaming of surface plasmon polaritons from a metallic nanochannels with defected surface cavity. *Microw Opt Technol Lett.* 2020;1–7. <https://doi.org/10.1002/mop.32325>